JST: Engineering and Technology for Sustainable Development
Volume 35, Issue 3, July 2025, 034-043

Effect of Temperature and Time on Crosslinking Reaction of Fabricating Modified Poly(Vinyl Alcohol) Materials for Pb(II) Removal in Aqueous Solutions

Truong Hoai Nam, Doan Thi Hoa Huyen, Nguyen Thi Thu Hang, Nguyen Vo Hong Ngoc, Tran Huy Trong, Do Kim Thanh, Nguyen Huu Tuan Minh, Vu Quynh Nhu, Tran Thi Luyen, Tran Quang Tung, Tran Thi Thuy*

Hanoi University of Science and Technology, Ha Noi, Vietnam
**Corresponding author email: thuy.tranthi3@hust.edu.vn*

Abstract

The study aims to evaluate the cross-linking ability of Poly(Vinyl Alcohol) (PVA) membranes with L-glutamic acid through solid-phase esterification reactions to improve water resistance. The cross-linked material exhibits enhanced Pb(II) ion adsorption capacity due to porosity introduced by Poly(Ethylene Glycol) (PEG), which increases surface area and swelling ability. The cross-linking reaction and porosity of the material were demonstrated by the crosslink density of the membrane and the material's swelling behavior in water. Results show that at 130 °C for 60 minutes, the optimal material was obtained, with a crosslink density of 92.89%. After the addition of PEG, water swelling increased to 131.77%, a 51% increase compared to the system containing only PVA and L-glutamic acid. The PVA-c-glu/PEG membrane exhibited excellent Pb(II) adsorption capacity, with a Q_e of 66.29 mg/g at room temperature (30 °C), an initial Pb(II) concentration of 114.08 mg/L, pH 7, and a material mass of 0.05 g in two days, compared to untreated PVA, which had a Q_e of 11.79 mg/g.

Keywords: Modified PVA, L-glutamic acid, Poly(Ethylene Glycol), cross-linked, heavy metal adsorption, Pb(II).

1. Introduction

Currently, with the rapid development of industry, agriculture, and services, water pollution is becoming increasingly severe, particularly concerning heavy metal contamination. This is an urgent challenge that has a significant impact on both the environment and public health. Common heavy metals include mercury (Hg), lead (Pb), cadmium (Cd), arsenic (As), chromium (Cr), and nickel (Ni) [1-4]. Heavy metal pollution commonly occurs in water basins near industrial zones, large cities, and mining areas. A characteristic of this pollution is the high concentration of metals in the water, leading to mass die-offs of fish and aquatic organisms. This poses a significant threat to the habitats of wildlife and human health [4, 5].

Pb(II), or lead (II), is a common form of lead in the environment and can cause severe impacts on both ecosystems and human health. In aquatic environments, Pb(II) can accumulate in the bodies of aquatic organisms, leading to physiological disorders and reduced reproductive capacity [6, 7]. When humans are exposed to Pb(II) through food, drinking water, or air, lead can accumulate in the body, leading to neurological, renal, and cardiovascular issues. Children are particularly sensitive to the toxicity of Pb(II), which can result in developmental delays and behavioral problems [6]. Therefore, controlling and reducing Pb(II) emissions into the environment is crucial for protecting public health and ensuring the sustainability of ecosystem.

Several major methods used for heavy metal removal include precipitation, ion exchange, electrochemical methods, and redox processes [8-11]. However, these methods often have several disadvantages, such as poor selectivity, the generation of by-products, and the lengthy time required to remove metals [12]. Currently, heavy metal adsorption is considered one of the most ideal and widely used methods. It meets requirements such as ease of management, simple operation, high efficiency, fast chemical kinetics, and additionally, it is cost-effective and meets technological demands.

Poly(Vinyl Alcohol) (PVA) is a polymer capable of film formation. Additionally, its main chain contains -OH groups that have the potential to adsorb heavy metals. As a result, PVA has garnered significant interest from both domestic and international researchers for the development of materials aimed at heavy metal adsorption and removal [13]. Furthermore, PVA is a non-toxic polymer that exhibits stability across various pH environments and possesses biodegradable properties. However, PVA is a linear polymer that contains a high density of

ISSN 2734-9381
https://doi.org/10.51316/jst.183.etsd.2025.35.3.5
Received: Sep 24, 2024; revised: Oct 29, 2024
accepted: Nov 22, 2024

hydrophilic -OH groups, which results in its poor mechanical strength in aqueous environments [13-15]. To address this issue, research focused on enhancing the mechanical strength and heavy metal adsorption capacity of PVA using crosslinking agents has attracted considerable interest from researchers. In this study, we employed L-glutamic acid as a crosslinking agent to form crosslinks in the PVA membrane, thereby improving the mechanical strength of PVA in aqueous environments. Additionally, the L-glutamic acid backbone contains -NH_2 groups, which are known to possess superior heavy metal adsorption capabilities compared to the -OH groups of PVA. Therefore, L-glutamic acid represents an ideal and environmentally friendly crosslinking agent.

However, the crosslinking of the PVA membrane results in a reduction of the free volume within the material's structure, as the PVA chains are closely packed together, thereby diminishing the permeability of water through the membrane. To address this drawback, we incorporated Poly(Ethylene Glycol) (PEG) to create porous structures in the material, leveraging the phase separation capability between PEG and PVA when the PEG content exceeds 20% relative to PVA [16], the regions previously occupied by PEG in the membrane will result in pores after its removal, to increase the surface area, thereby enhancing the contact between the metal and the material, and to increase the free volume within the material's structure.

The objective of this study was to investigate the effects of temperature and reaction time on the crosslinking between PVA and L-glutamic acid, aiming to enhance the mechanical stability of PVA in water by measuring crosslinking density within the membrane. Additionally, the study examined the swelling degree of the membrane after adding PEG as an agent to create pores, increasing the membrane's contact area with the solution for potential applications in the adsorption and removal of heavy metals, specifically Pb(II), from solutions.

2. Experiments

2.1. Chemicals

Poly(Vinyl Alcohol) (CAS: 900289-5) (degree of hydrolysis, 99%) was purchased from Sigma-Aldrich (USA). L-glutamic acid (CAS: 1002910250) was purchased from Merck (Germany). Poly(Ethylene Glycol) (CAS: 25322-68-3) (Mw = 5500 – 7000) was provided by Sigma-Aldrich (USA). Lead(II) Nitrate (CAS: 10099-74-8) (assay ≥ 99.0%) and 4-(pyridylazo)-resorcinol (PAR) (CAS: 1141-59-9) (assay ≥ 98.0%) were purchased from Merck (Germany). Other chemical were also provided by Sigma-Aldrich (USA) and Merck (Germany).

2.2. Materials

2.2.1. Synthesis of PVA-c-glu material

As summarized in Fig. 1. PVA was dissolved in distilled water and stirred at 140 °C at 350 rpm until it was completely dissolved. L-glutamic acid was dissolved in distilled water and stirred at room temperature for 1 hour. Subsequently, the PVA and L-glutamic acid solutions were mixed and stirred at 50 °C at 350 rpm for 2 hours until a homogeneous solution was achieved, resulting in a mixture containing PVA and L-glutamic acid. The mixture was poured into a Petri dish and dried at 50 °C until it was completely dry, yielding a crude PVA-c-glu membrane without crosslinking. After drying, the membrane was subjected to a crosslinking reaction at a temperature of x °C (x = 100; 110; 120; 130; 140; 150) for a duration of y minutes (y = 30; 60; 90; 120; 150), resulting in the PVA-c-glu membrane.

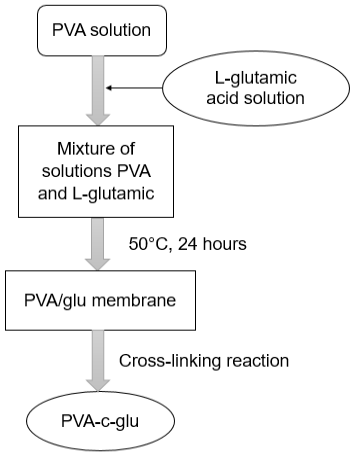

Fig. 1. Schematic summary of the PVA-c-glu material synthesis process

2.2.2. Synthesis of PVA-c-glu/PEG material

As summarized in Fig. 2. PVA was dissolved in distilled water and stirred at 140 °C at 350 rpm until it was completely dissolved. L-glutamic acid and PEG were dissolved in distilled water and stirred at room temperature for 1 hour. Subsequently, the PVA, L-glutamic acid, and PEG solutions were mixed and stirred at 50 °C at 350 rpm for 2 hours until a homogeneous solution was achieved, resulting in a mixture containing PVA, L-glutamic acid, and PEG. The mixture was poured into a silicone dish and dried at 50 °C until it was completely dry, yielding a crude PVA-c-glu/PEG membrane. After drying, the membrane was subjected to a crosslinking reaction at a temperature of x °C (x = 100; 110; 120; 130; 140; 150) for a duration of y minutes (y = 30; 60; 90; 120; 150), resulting in the PVA-c-glu/PEG membrane.

After the crosslinking reaction, the membrane was extracted to remove any unreacted PEG and L-glutamic acid by immersing it in distilled water at room temperature (30 °C) for 2 days.

Then, the extracted membrane was dried at 50 °C until it was completely dry, yielding the PVA-c-glu/PEG membrane.

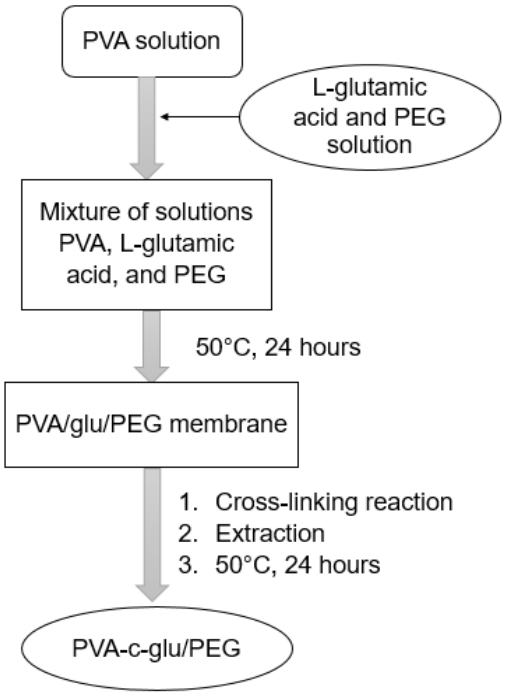

Fig. 2. Schematic summary of the PVA-c-glu/PEG material synthesis process

2.3. Working Solution

The standard Pb(II) solution was prepared by dissolving $Pb(NO_3)_2$ in distilled water to achieve a concentration of 154.00 mg/L. Experimental solutions with varying Pb(II) concentrations were prepared by diluting the standard Pb(II) solution.

The working solution was freshly prepared daily, consisting of 2.0 mL of the working solution, 2.0 mL of KNO_3 solution, and 2.5 mL of 4-(pyridylazo)-resorcinol (PAR) solution, which was then adjusted to a pH of 9.5. The absorbance of the colored solution was measured using a UV-Vis spectrophotometer at the maximum wavelength (λ_{max}) of 525 nm (Fig. 3). The concentration of Pb(II) in the solution was determined using the Lambert-Beer law, expressed by the following equation:

$$A = \varepsilon \times b \times C \quad (1)$$

where: A is the absorbance, ε is the molar absorptivity constant, b is the path length of the cuvette (b = 1 cm), and C is the concentration of Pb(II) in the solution.

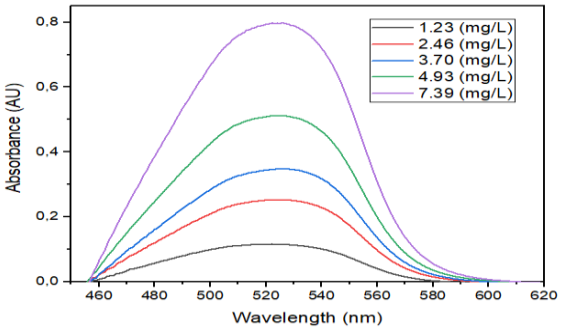

Fig. 3. The standard peak absorbance signal

2.4. Methods

2.4.1. Investigation of crosslinking density

x (g) of the sample (W_0) was soaked in distilled water for 5 hours at a temperature of 90 °C and stirred at a speed of 300 rpm. Afterward, the sample was removed and thoroughly rinsed with distilled water to eliminate any dissolved components and then dried at 50 °C until the material's mass showed minimal change after drying (W_d). The difference in mass before and after testing indicated the reaction capability between PVA and L-glutamic acid; unreacted portions dissolved at high temperatures and were washed away from the material. The experiment was repeated multiple times, and the results were averaged. The crosslinking density formed was calculated using the following formula:

$$\textit{Crosslinking density}\ (\%) = \frac{W_d}{W_0} \times 100 \quad (2)$$

where: W_d is the mass of the material after the investigation (g), and W_0 is the initial mass of the material before the investigation (g)

2.4.2. Investigation of water swelling

The dry material with an initial mass (m_0) was immersed in a 1L glass beaker filled with distilled water, stirred at a speed of 250 rpm, and maintained at room temperature (30 °C). After 24 hours, the material was removed, and excess surface water was eliminated until no droplets remained visible. The post-experiment mass (m_1) was then recorded. The mass difference before and after swelling indicated the material's capacity to allow water to permeate and retained within the membrane. The experiment was repeated multiple times, and the results were averaged.

The water swelling ratio of the material was calculated using the following formula:

$$\textit{Water swelling}\ (\%) = \frac{m_1 - m_0}{m_0} \times 100 \quad (3)$$

where: m_1 is the mass of the material after swelling investigation (g), and m_0 is the initial mass of the material (g).

2.4.3. Effect of pH on the adsorption capacity of the material

0.10 g of the material was added into a beaker containing 50 mL of Pb(II) solution at a concentration of 74.00 mg/L, along with 20 mL of buffer solution with pH ranging from 3 to 9. The mixture was stirred at a speed of 100 rpm, and the adsorption of the samples was carried out for the determined investigation period. Afterward, the concentration of the solution was measured using a UV-Vis spectrophotometer (Agilent 8543).

2.4.4. Effect of membrane mass on adsorption capacity

x (g) of the material (where *x* = 0.05; 0.10; 0.20; 0.30; 0.40; 0.50) was added into a beaker containing 50 mL of Pb(II) solution at a concentration of 85.23 mg/L, along with 20 mL of buffer solution at pH 7 (previously investigated in section 2.3.3). The mixture was stirred at a speed of 100 rpm and perform adsorption for a specified duration. Afterward, the concentration of the solution was measured using a UV-Vis spectrophotometer

2.4.5. Effect of adsorption time on adsorption capacity

0.05 g of the material (previously investigated in section 2.3.4) was added into a beaker containing 50 mL of Pb(II) solution at a concentration of 85.23 mg/L, along with 20 mL of buffer solution at pH 7. The mixture was stirred at a speed of 100 rpm. The experiment was conducted at different time intervals of 30, 60, 90, 120, 150, 180, and 210 minutes. Afterward, the concentration of the solution was measured using a UV-Vis spectrophotometer

2.4.6. Effect of Pb(II) metal concentration on adsorption capacity

0.05 g of the material was added into a beaker containing 50 mL of Pb(II) solution at a concentration of *x* (mg/L) (where *x* = 35.44; 46.38; 60.59; 74.00; 85.23; 99.43; 114.08; 128.47), along with 20 mL of buffer solution at pH 7. The mixture was stirred at a speed of 100 rpm. The experiment was conducted at specified time intervals. Afterward, the concentration of the solution was measured using a UV-Vis spectrophotometer

2.5. Adsorption Capacity of Pb(II)

Investigate the adsorption efficiency/adsorption capacity of the material under the conditions of pH, membrane mass, and time previously examined, conducted at room temperature (30 °C). The concentration of the solution after adsorption was measured using a UV-Vis spectrophotometer. Adsorption efficiency was calculated using the following formula (*H*%):

$$H(\%) = \frac{(C_0 - C_e)}{C_0} \times 100\ (\%) \quad (4)$$

Adsorption capacity (Q_e):

$$Q_e = \frac{(C_0 - C_e)}{W} \times V\ (\text{mg/g}) \quad (5)$$

where: C_0 is the initial metal concentration (mg/L); *Ce* is the remaining metal concentration in the solution (mg/L); *W* is the mass of the membrane being investigated (g); *V* is the total volume of the solution being investigated (L).

2.6. Characterization of Materials

The morphologies of the PVA, PVA-c-glu, and PVA-c-glu/PEG films were examined using a scanning electron microscope (SEM) from Thermo Fisher Scientific (USA) at an accelerating voltage of 15 kV.

3. Result and Discussion

3.1. Confirmation of the Structure Morphology of the PVA Membrane Porousified by PEG

Based on the surface morphology analysis results of the materials (Fig. 4a and Fig. 4b), it was observed that both the PVA and PVA-c-glu materials exhibited smooth and planar surfaces. This indicated that the PVA and PVA-c-glu membranes possessed a dense and continuous internal structure.

However, after the addition of PEG, the internal structure of the material changed significantly, resulting in a surface with an uneven texture and the appearance of pores. Fig. 4c showed that the membrane surface featured irregularly shaped pores of varying sizes, ranging from 30 to 260 μm. This demonstrated that the incorporation of PEG into the material created porous structures on the surface, which increased the surface area of the membrane.

3.2. Effect of Reaction Temperature on Crosslinking Density and Swelling Behavior of PVA-c-glu Material

Within the temperature range of 100 to 130 °C, the crosslinking density of the material increased, indicating an enhanced reaction between PVA and L-glutamic acid that forms crosslinks in the material. However, when the temperature rose from 130 to 150 °C, the crosslinking density in the membrane decreases (Fig. 5a). This could be explained by the fact that at high temperatures (above 130 °C), L-glutamic acid undergoes dehydration, leading to intramolecular cyclization, whereby L-glutamic acid was converted to pyroglutamic acid. This conversion reduced the amount of glutamic acid available for the reaction, resulting in a decreased crosslinking density in the membrane [17].

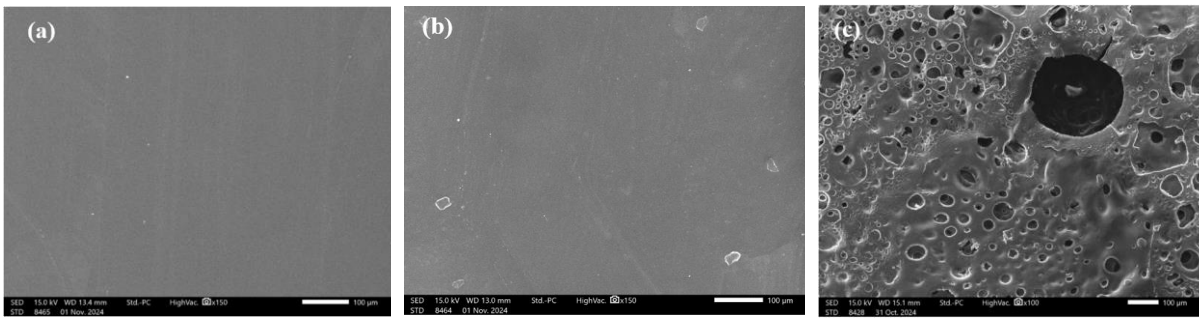

Fig. 4. Surface morphology results of the materials: (a) PVA; (b) PVA-c-glu; (c) PVA-c-glu/PEG

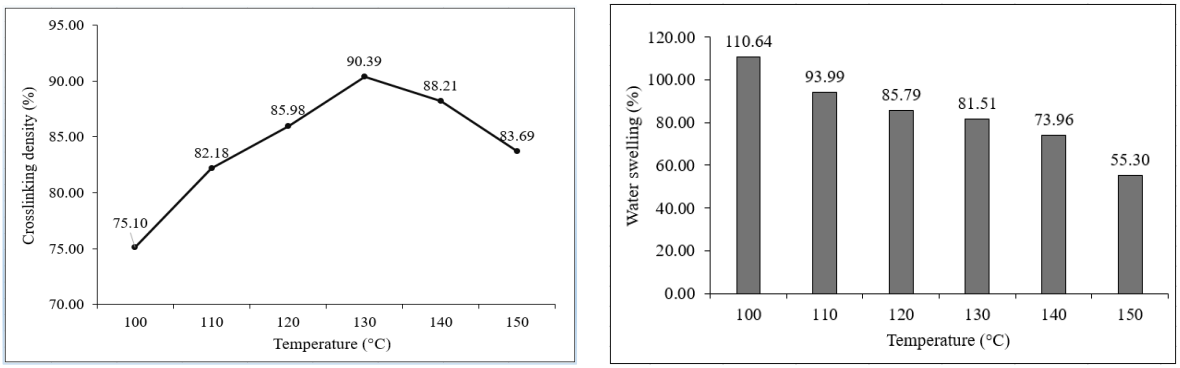

(a) (b)

Fig. 5. (a) Effect of reaction temperature on crosslinking density of the membrane, (b) Effect of reaction temperature on membrane water swelling

When the crosslinking density in the membrane increased, it caused the polymer chains to be linked into a dense network, simultaneously reducing the -OH groups in the membrane. This made it more difficult for water to permeate through the membrane and to be retained within the membrane, resulting in a decrease in the swelling behavior of the membrane (Fig. 5b).

However, from 130 to 150 °C, although the crosslinking density decreased, the water swelling of the material continued to decrease. This could be explained by the fact that at higher temperatures, the functional groups in the polymer became less sensitive to water. (During the thermal curing process, some functional groups changed their chemical states, hydroxyl groups -OH formed hydrogen bonds with each other or with other groups in the polymer structure, thereby reducing their interaction with water [18-20]).

Additionally, polymers that have been thermally cured generally exhibited higher thermal stability. As the temperature increased, the swelling due to water infiltration also decreased, as the material maintains a more stable structure and did not deform as it did at lower temperatures (the chains within the polymer membrane became stiffer and more difficult to move, resulting in reduced chain mobility).

3.3. Effect of Reaction Time on Crosslinking Density and Swelling Behavior of PVA-c-glu Material

When the crosslinking reaction time was increased from 30 to 60 minutes, the crosslinking density increased significantly. However, when the time was extended from 60 to 150 minutes, the crosslinking density of the membrane tended to stabilize (Fig. 6a). This could be explained by the fact that at this point, PVA and L-glutamic acid had reacted completely, and no further crosslink reactions occurred. As the crosslinking reaction time increased from 30 to 60 minutes, the water swelling of the membrane decreased. This was due to the rapid formation of crosslinks within the membrane, resulting in a dense network that made it more difficult for water to permeate through the membrane, corresponding to the increase in crosslinking density during the reaction period from 30 to 60 minutes (Fig. 6b).

However, when the reaction time continued to increase from 120 to 150 minutes, the water swelling continues to decrease. This was also due to the prolonged reaction time, which enhanced the rigidity of the membrane, making it stiffer. The polymer chains within the membrane became less mobile and more difficult to move, resulting in reduced water permeability through the membrane, thereby decreasing the swelling behavior of the membrane.

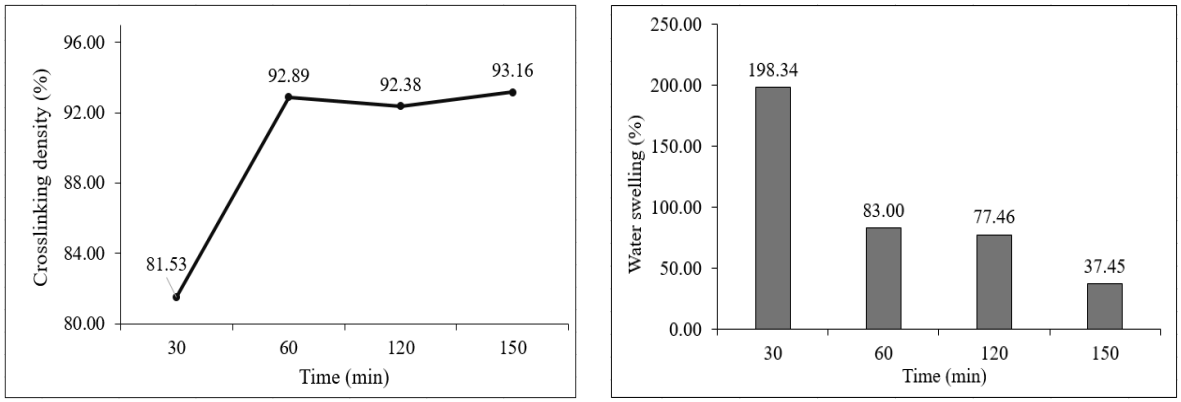

(a) (b)

Fig. 6. (a) Effect of reaction time on the crosslinking density of the membrane, (b) Effect of reaction time on the swelling behavior of the PVA-c-glu membrane

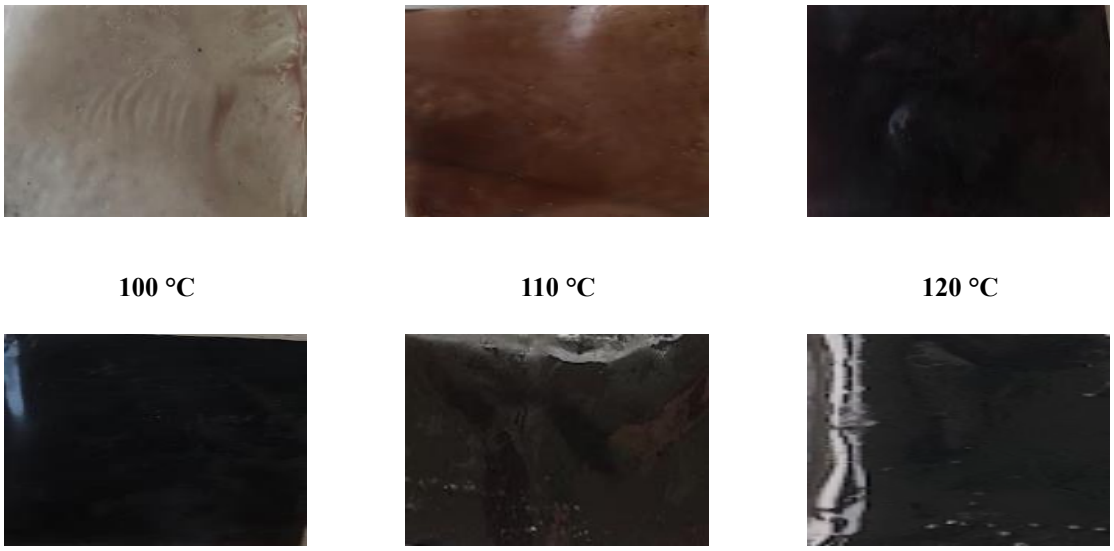

100 °C **110 °C** **120 °C**

130 °C **140 °C** **150 °C**

Fig. 7. The PVA-c-glu material investigated at various crosslinking reaction temperatures

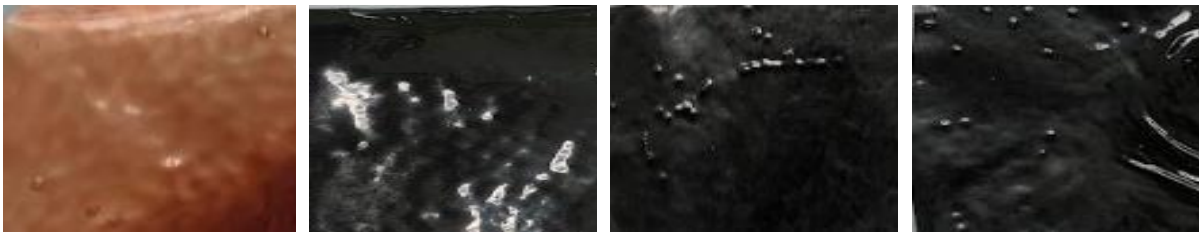

30 min **60 min** **120 min** **150 min**

Fig. 8. The PVA-c-glu material investigated at various crosslinking reaction times

From the results of Fig. 7 and Fig. 8, it was evident that the material underwent color changes when the factors of time and temperature were varied, which in turn affects the crosslinking ability of the material. This also demonstrated that the impact of temperature and time on the crosslinking reaction was crucial.

When the temperature increased (Fig. 7), it could be observed that from 100 to 120 °C, the color changed significantly. However, between 120 and 150 °C, the color of the material remained almost the same, showing no notable change.

Similarly, when the reaction time was extended from 30 to 60 minutes, the material's color changes noticeably. When the time was further extended from 60 to 120 minutes, the color did not change significantly (Fig. 8).

3.4. Effect of Temperature and Reaction Time on the Swelling Behavior of PVA-c-glu/PEG Material

When the material was supplemented with PEG, which acted as a porogen to increase the surface area of the membrane, this led to an increased contact area between the membrane and water.

Additionally, PEG facilitated the easier ingress of water into the membrane, resulting in a significant increase in the water swelling of the PVA-c-glu/PEG material compared to the conventional modified material, PVA-c-glu (Fig. 9).

With both factors affecting the crosslinking reaction including reaction time and reaction temperature, the swelling behavior shows a similar decreasing trend as that of PVA-c-glu material.

However, the PEG-containing material consistently exhibits a significantly greater swelling degree than the PVA-c-glu counterpart, highlighting the beneficial role of PEG in improving water uptake.

3.5. Comparison of Pb(II) Adsorption Capacity of PVA-c-glu and PVA-c-glu/PEG Materials

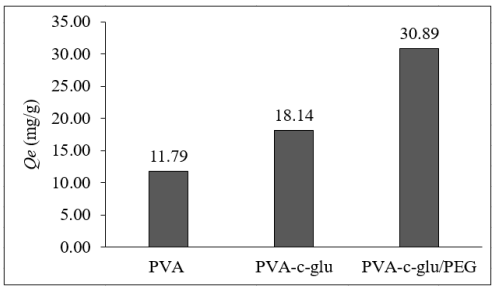

Fig. 10. Adsorption capacity (Q_e) of PVA, PVA-c-glu, and PVA-c-glu/PEG membranes

From Fig. 10, it could be observed that when crosslinking had not yet been performed, the adsorption capacity of Pb(II) by the PVA membrane was quite low, with a value of Q_e = 11.79 mg/g. This was because, in the absence of crosslinking with L-glutamic acid, only the -OH functional groups in the PVA molecular chain were responsible for complexation with Pb(II) ions. When L-glutamic acid was introduced and crosslinking occurred to form the PVA-c-glu membrane, the adsorption capacity for Pb(II) significantly increased from 11.79 mg/g to 18.14 mg/g. This increase in Q_e was due to the addition of L-glutamic acid, which introduces the -NH_2 group alongside the existing -OH groups on the PVA chain that complex with Pb(II). The nitrogen atom (N) has a lower electronegativity than oxygen (O), made the lone electron pair on N from the -NH_2 group more readily available to participate in coordinate bonding with Pb(II) ions. N could donate the lone electron pair more effectively than O, making it a stronger ligand for complexation with Pb(II) ions. Consequently, the complexation ability of the -NH_2 group with Pb(II) was superior to that of the -OH group.

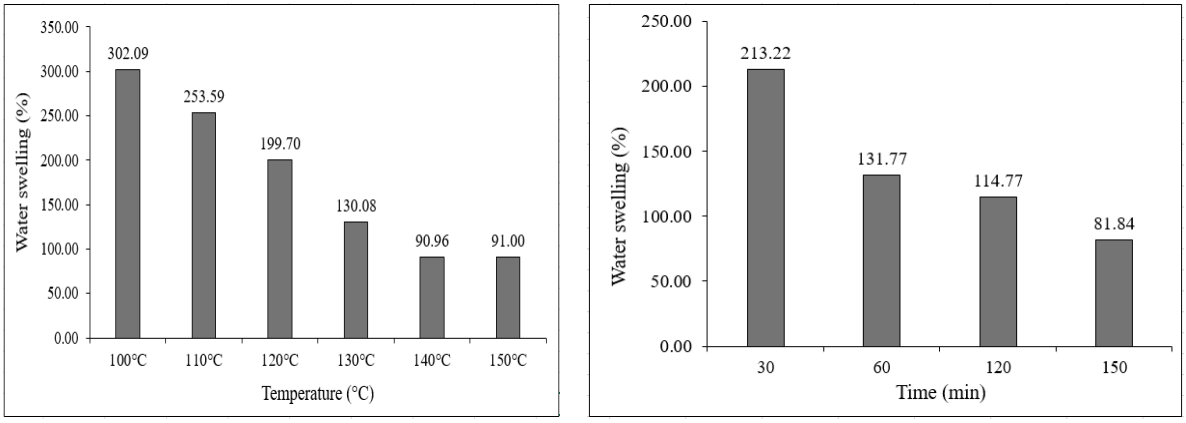

(a) (b)

Fig. 9. Effect of temperature and reaction time on the swelling behavior of the PVA-c-glu/PEG membrane: a) Temperature, b) Time

When PEG was added to the material membrane, the Q_e value of the material reached 30.89 mg/g, which was a significant increase compared to the PVA material that only crosslinks with L-glutamic acid. The presence of pores within the material enhanced its water swelling capacity upon the addition of PEG, thereby increasing the free volume of the material. Additionally, the formation of pores increased the surface area of the material in contact with Pb(II), enhancing the interaction of the functional groups within the membrane with Pb(II).

3.6. Effect of pH on the Adsorption Capacity of the Material

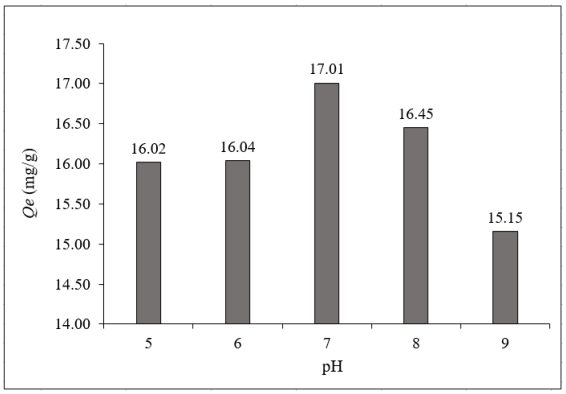

Fig. 11. Effect of pH on the adsorption capacity of PVA-c-glu/PEG

The results indicated that at a pH value of 7, the material exhibited the highest Q_e value, demonstrating its optimal adsorption capacity for Pb(II). As the pH of the adsorption solution increased from 5 to 7, the adsorption capacity of the material also rises, with Q_e increasing from 16.02 to 17.01 mg/L. This could be explained by the fact that in an acidic environment, the functional groups of the material became protonated, acquiring a positive charge. Consequently, this resulted in the same charge as Pb(II), thereby reducing the adsorption capacity for the metal.

As the pH value continued to increase from 7 to 9, the adsorption capacity of the material for Pb(II) decreased, with the Q_e value dropping from 17.01 to 15.15 mg/L (Fig. 11). This could be explained by the fact that in a basic environment, Pb(II) tended to form complexes with free -OH ions present in the solution, leading to a reduction in the amount of Pb(II) available for adsorption by the material.

3.7. Effect of Material Mass on the Adsorption Capacity of the Material

From the results of the investigation on the effect of adsorbent mass (Fig. 12), it was observed that as the mass of the adsorbent increased, the percentage of Pb(II) adsorption rises from 34.76% to 40.39%. However, the adsorption capacity (Q_e) decreased from 32.44 mg/g to 4.14 mg/g. This decrease in Q_e was attributed to the fact that while the mass of the adsorbent increases, the concentration of Pb(II) in the solution remained unchanged. The number of available functional groups capable of adsorbing Pb(II) was not fully utilized, and the concentration of Pb(II) had already been reduced due to prior adsorption. This resulted in the adsorption process shifting towards desorption.

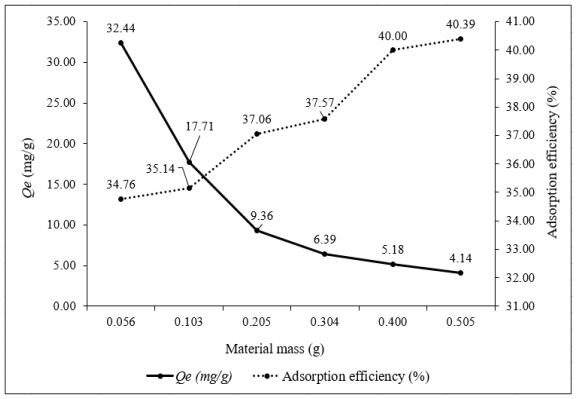

Fig. 12. Effect of material mass on the adsorption capacity of the material

3.8. Effect of Time on the Adsorption Capacity of the Material

From Fig. 13, it was observed that the adsorption capacity (Q_e) increased from day 1 to day 2. From day 2 to day 4, the value of Q_e changed insignificantly, indicating that the adsorption process reached equilibrium by the second day.

In the initial phase, from the first day of adsorption to the second day, the adsorption rate increases sharply. This was attributed to the large number of available functional groups that were ready to interact with Pb(II) ions at the beginning of the adsorption process, resulting in rapid and efficient adsorption.

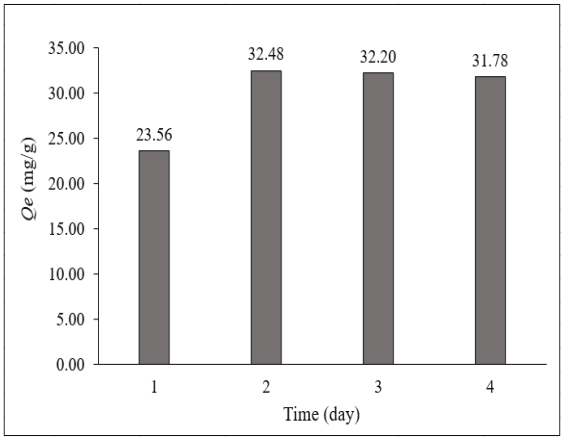

Fig. 13. Effect of time on the adsorption capacity of the material

However, from the second adsorption day onward, the adsorption rate reached equilibrium, with the value of Q_e changing insignificantly. This was due to the membrane that had participated in the complexation process with Pb(II) ions. As the number of free functional groups in the material decreased, the adsorption capacity of the material diminishes, leading to a state of balance. Consequently, there was little variation in the value of Q_e, which reflected the equilibrium of the adsorption process.

3.9. Effect of Pb(II) Concentration on the Adsorption Capacity of the Material

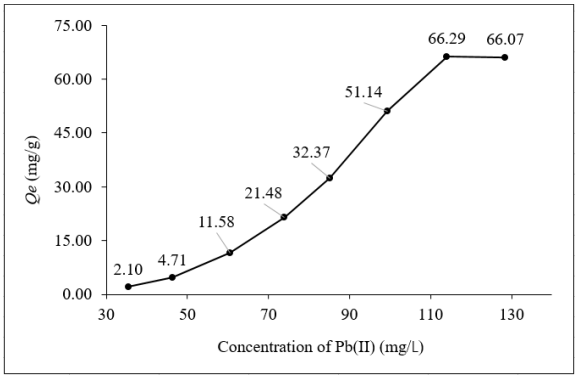

Fig. 14. Effect of Pb(II) concentration on the adsorption capacity of the material

From the results (Fig. 14), it was evident that as the concentration increased from 35.44 to 114.08 mg/L, the value of Q_e for the material increased from 2.10 to 66.29 mg/g. However, when the concentration reached 128.47 mg/L, the value of Q_e changes insignificantly, indicating that the adsorption process had reached equilibrium. This demonstrated that the material achieved maximum adsorption capacity at a Pb(II) concentration of 114.08 mg/L with an adsorbent mass of 0.05 g.

4. Conclusions

At a temperature of 130 °C and a reaction time of 60 minutes, the crosslinking reaction between PVA and L-glutamic acid achieved optimal conditions, resulting in a crosslinking density of approximately 92.89%. Furthermore, the addition of PEG as a porogenic agent significantly enhanced the adsorption capacity of the material, with the swelling degree of the PVA-c-glu/PEG membrane reaching 131.77%, an increase of approximately 51% compared to the PVA-c-glu material.

The PVA-c-glu/PEG material exhibited excellent adsorption capacity for Pb(II) ions, achieving a maximum Q_e value of 66.29 mg/g at room temperature (30 °C). This performance was observed with an initial Pb(II) concentration of 114.08 mg/L, a solution pH of 7, and an adsorbent mass of 0.05 g over a maximum adsorption duration of 2 days.

Acknowledgements

This research is funded by the Ministry of Education and Training of Vietnam under the grant number B2024-BKA-05.

References

[1] Mahurpawar M, Effects of heavy metals on human health, International Journal of Research - Granthaalayah, vol. 3, iss. 9, pp. 1-7, Sep. 2015. https://doi.org/10.29121/granthaalayah.v3.i9SE.2015.3282

[2] Roy S, Gupta S K, Prakash J, Habib G., and Kumar P, A global perspective of the current state of heavy metal contamination in road dust, Environmental Science and Pollution Research, vol. 29, pp. 33230-33251, Jan. 2022. https://doi.org/10.1007/s11356-022-18583-7

[3] Rashid A, Schutte B J, Ulery A, Deyholos M K, Sanogo S, Lehnhoff E A and Beck L, Heavy metal contamination in agricultural soil: environmental pollutants affecting crop health, Agronomy, vol. 13, iss. 6, May 2023. https://doi.org/10.3390/agronomy13061521

[4] Sharifi S A, Zaeimdar M, Jozi S A, and Hejazi R, Effects of soil, water and air pollution with heavy metal ions around lead and mining and processing factories, Water, Air, & Soil Pollution, vol. 234, 2023. https://doi.org/10.1007/s11270-023-06758-y

[5] Jiwan S and Ajay, Effects of heavy metals on soil, plants, human health and aquatic life, International Journal of Research in Chemistry and Environment, vol. 1, pp. 15-21, Oct. 2011.

[6] Collin S, Baskar A, Geevarghese D M, Ali M N V S, Bahubali P, Choudhary R, Lvov V, Tovar G I, Senatov F, Koppala S, and Swamiappan S, Bioaccumulation of lead (Pb) and its effects in plants: a review, Journal of Hazardous Materials Letters, Nov. 2022. https://doi.org/10.1016/j.hazl.2022.100064

[7] Dikhanbaevna B A, Tazhmahanbetovich Z K, Duysenbaevna K G, Nikolaevich B V and Dzhanabaevna M A , Influence of heavy metals on the environment and methods of soil bioremediation control, International Journal of Engineering Research and Technology., vol. 13, no. 6, pp. 1120-1125, 2020. https://doi.org/10.37624/IJERT/13.6.2020.1120-1125

[8] Aguayo-Villarreal I A, Bonilla-Petriciolet A, and Muñiz-Valencia, Preparation of activated carbons from pecan nutshell and their application in the antagonistic adsorption of heavy metal ions, Journal of Molecular Liquids, vol. 230, pp. 686-695, Mar. 2017. https://doi.org/10.1016/j.molliq.2017.01.039

[9] Tang J, Xi J, Yu J, Chi R, and Chen J, Novel combined method of biosorption and chemical precipitation for recovery of Pb2+ from wastewater, Environmental Science and Pollution Research, vol. 25, pp. 28705-28712, Aug. 2018. https://doi.org/10.1007/s11356-018-2901-6

[10] Yang X, Liu L, Tan W, Liu C, Dang Z, and Qiu G, Remediation of heavy metal contaminated soils by

organic acid extraction and electrochemical adsorption, Environmental Pollution, vol. 264, pp. 1-9, Sep. 2020. https://doi.org/10.1016/j.envpol.2020.114745

[11] Deng S, Liu X, Liao J, Lin H, and Liu F, PEI modified multiwalled carbon nanotube as a novel additive in PAN nanofiber membrane for enhanced removal of heavy metal ions, Chemical Engineering Journal, vol. 375, Nov. 2019. https://doi.org/10.1016/j.cej.2019.122086

[12] Wang B, Lan J, Bo C, Gong B, and Ou J, Adsorption of heavy metal onto biomass-derived activated carbon: review, RSC Advances, vol. 13, iss.7, pp. 4275-4302, Jan. 2023. https://doi.org/10.1039/D2RA07911A

[13] Aslam M, Kalyar M A, and Raza Z A, Polyvinyl alcohol: a review of research status and use of polyvinyl alcohol based nanocomposites, Polymer Engineering and Science, vol. 58, iss. 12, pp. 2119-2132, Dec. 2018. https://doi.org/10.1002/pen.24855

[14] Vu Trung N, Pham Thi N, Nguyen T H, Nguyen M N, Tran Anh D, Nguyen Trung T, Tran Quang T, Than Van H, and Tran Thi T, Tuning the thermal and mechanical properties of poly(vinyl alcohol) with 2,5-furandicarboxylic acid acting as a biobased crosslinking agent, Polymer Journal, vol. 54, pp. 335-343, 2022. https://doi.org/10.1038/s41428-021-00583-y

[15] Pham Thi N, Ho L H T, Vu Trung N, Tran H A, Nguyen Ngoc M, Nguyen Thu H, Le Quang D, and Tran Thi T, Investigation of the effects of cellulose nanofiber on the properties of poly(vinyl alcohol) crosslinked by 2,5-furandicarboxylic acid, Journal of Elastomers & Plastics, vol. 56, pp. 194-210, Jan. 2024. https://doi.org/10.1177/00952443231226420

[16] Falqi F H, Bin-Dahman O A, Hussain M and Al-Harthi, Preparation of miscible PVA/PEG blends and effect of graphene concentration on thermal, crystallization, morphological, and mechanical properties of PVA/PEG (10 wt%) blend, International Journal of Polymer Science, vol. 2018, pp. 1-10, Sep. 2018. https://doi.org/10.1155/2018/8527693

[17] Zhu Z, Bian Y, Zhang X, Zeng R, and Yang B, Terahertz spectroscopy of temperature-induced transformation between glutamic acid, pyroglutamic acid and racemic pyroglutamic acid, Spectrochimica Acta Part A: Molecular and Biomolecular Spectroscopy, vol. 275, pp. 121-150, Jul. 2022. https://doi.org/10.1016/j.saa.2022.121150

[18] H. Li, W. Zhang, W. Xu, and X. Zhang, Hydrogen bonding governs the elastic properties of poly (vinyl alcohol) in water: single-molecule force spectroscopic studies of PVA by AFM, Macromolecules, vol. 33, no. 2, pp. 465-469, 2000. https://doi.org/10.1021/ma990878e

[19] H. S. Mansur, R. L. Oréfice, and A. A. Mansur, Characterization of poly (vinyl alcohol)/poly (ethylene glycol) hydrogels and PVA-derived hybrids by small-angle X-ray scattering and FTIR spectroscopy, Polymer, vol. 45, no. 21, pp. 7193-7202, 2004. https://doi.org/10.1016/j.polymer.2004.08.036

[20] J. A. Venegas-Sánchez, M. Tagaya, and T. Kobayashi, Ultrasound stimulus inducing change in hydrogen bonded crosslinking of aqueous polyvinyl alcohols, Ultrasonics Sonochemistry, vol. 21, no. 1, pp. 295-309, 2014. https://doi.org/10.1016/j.ultsonch.2013.06.011